International Journal of Computational and Experimental Science and ENgineering (IJCESEN)

Vol. 10-No.4 (2024) pp. 1311-1319

http://www.ijcesen.com

ISSN: 2149-9144

Research Article

An efficient approach for detecting downsyndrome fetus images using deep learning method

V. Gokulakrishnan[1], S. Selvakumar[2,*]

[1]Research Scholar, Department of Computer Science and Engineering, Dhanalakshmi Srinivasan University, Tiruchirappalli, Tamil Nadu, India.
Email: gokulakrishnanv.phd2022@dsuniversity.ac.in - **ORCID:** 0009-0003-9115-7969.

[2]Professor, Department of Computer Science and Engineering, Dhanalakshmi Srinivasan University, Tiruchirappalli, Tamil Nadu, India.
* **Corresponding Author Email:** ssksri@gmail.com - **ORCID:** 0009-0005-9820-3387.

Article Info:

DOI: 10.22400/ijcesen.705
Received : 30 November 2024
Accepted : 02 December 2024

Keywords :

Fetus,
Down syndrome,
dataset,
deep learning,
Nasal bone.

Abstract:

Down Syndrome (DS) is the genetical disorder which can be screened by the ultrasound fetus images. This research work proposes an automated ultrasound fetus image classification system using DL algorithm. This proposed system receives the source ultrasound fetus image and the spatial domain pixels in this image have been converted into multi modal domain pixels using Gabor wavelet. Further, Local Binary Pattern (LBP) has been computed from the multi domain image and these values have been fed into the proposed DL architecture to classify the source fetus image into either normal fetus or abnormal fetus. The morphological algorithm have been used on the abnormal fetus images in order to locate the Nasal Bone (NB) and this proposed DS detection method has been tested on two independent fetus ultrasound datasets Mendeley and Fetal Medicine Foundation (FMF). The proposed NT region segmentation system attains 98.44% NBSe, 98.63% NBSp and 98.62% NBAcc, for the set of 10 fetus images from the Mendeley dataset in this work. The proposed NB region segmentation system attains 98.67% NBSe, 98.66% NBSp and 98.66% NBAcc, for the set of 10 fetus images from the FMF dataset in this work.

1. Introduction

The growth delays in fetus of the human causes the genetic disorder which is known as Down Syndrome (DS) or Trisomy 21. The intellectual disability due to chromosome disorder is the main reason for occuring DS. If the DS is screened at an earlier stage in the pregnancy period of 11-14 weeks, the fetus can be aborted in order to prevent the DS affected birth. Hence, the earlier detection and screening of the DS in fetus stage is very important. The DS in fetus can be detected using any of the two methods as Nuchal Translucency (NT) analysis way and another one is to analyze the morphological properties of the nasal bone in fetus. The NT measures the amount of fluid-filled space behind an unborn baby's neck. The scan is usually performed between 11+2 and 14+1 weeks of pregnancy [1-4]. By detecting and analyzing the NT region in fetus, the DS can be screened at an earlier stage. The nasal bone length in fetuses with Down syndrome is below the 5th percentile in a significantly higher proportion than in normal fetuses. The ratio of nasal bone to nasal tip length (NB/NL) is also a diagnostic tool for Down syndrome. In fetuses with Down syndrome, the NB/NL ratio is 1/3 or below in 35.5% of cases, compared to 1.3% in euploid fetuses. By detecting and analyzing the length of the nasal bone in fetus, the DS can be screened at an earlier stage. In this paper, the fetus images are obtained by the ultrasound scanning method and these fetus images are used to detect the nasal bone for DS early stage detection process [5-9].

Figure 1 is the ultrasound fetus with DS in which the nasal bone is not available. Mostly, machine learning systematic algorithms have been used for screening the DS in fetus. Though these machine learning based systematic algorithms are effective in nature, the detection of DS rate using fetus with the aid of the machine learning systematic algorithms are low. Hence, the Deep Learning (DL) algorithms have been used for detecting the normal

***Figure 1**. DS fetus (absense of nasal bone)*

fetus (with nasal bone) and the abnormal fetsu (without nasal bone).

This paper has been structured as section 2 states the tradional DS detection methods using ultrasound fetus images, section 3 presents the novel and efficient DS detection methods using DL algorithms and the simulation results are elloborated in section 4 and finally the conclusion is stated in section 5.

2. Literature survey

Tamilarasi et al. [6] presented a technique that achieved 98.9% accuracy in the detection and segmentation of glioma tumors by combining a Non-Subsampled Shearlet Transform with a UNet CNN methodology. Aijaz Ahmad Reshi et al. [8] implemented deep learning modelling algorithms for the earlier detection of DS in fetus images. The concurrency complexity of this DL algorithms have been significantly reduced in this paper by avaoiding the overfitting errors during the features processing between the inbuilt layers in the DL algorithm. This method has been tested with large number of fetus images with DS case and the fetus images without DS case. The authors obtained 97% of average DS detection rate in ultrasound fetus images. The k-mean clustering procedure was used by Thiyaneswaran et al. [9] to identify and segment cancer parts in skin images, and they achieved an average accuracy of 90.0%. Chengyu Wang et al. [10] predicted and analyzed the DS assessment using swin transformation model and the modified deep learning architecture. This swin transformation decomposed the ultrasound fetus image into number reliable and stable coefficients. These swin transformed set of coefficients were classified by the linear binary classification algorithm in this work. The authors obtained 96% of average DS detection rate in ultrasound fetus images. Further, the k-fold validation approximation algorithm was used in this work to validate the DS detection rate with respect to various set of test fetus ultrasound images. In order to segment the cancer portion of cervical images, Elayaraja et al. [12] created a GA-based convolutional neural networks methodology that yields 99.36% of standard AC (accuracy). Phung et al. [13] designed and proposed a multi branch CNN architectural model to predict the DS in ultrasound fetus imges. This multi branch CNN had the inheritance logical propertis by the internal layers in this architecture. This proposed multi branch CNN architecture has been constituted with the lower order and higher order branch, where the lower order branch consisted with lower kernels and the higher order branch consisted with higher kernels to obtain the higher DS detection index rate. This multi branch CNN architecture has been tested on various sources of ultrasound fetus images and the results were well compared with various validation model results in this paper. Senthil Kumar T et al. [14] increased accuracy by employing a technique that involved image thickening and backdrop thinning to extract performance assessment metrics.

Thomas et al. [11] used NT segmented region in ultrasound fetus image in ordet to evlaute the DS detection index. By analyzing the morphological parameters from the segmented NT region in ultrasound fetus images, the fetus images were classified into various categories such as normal or abnormal. An Adaptive Neuro-Fuzzy Inference System (ANFIS) classification approach was suggested by Kumarganesh et al. [15] for the categorization of cancers from the base pictures [10-15]. Their accuracy in cancer segmentation was 97.63%. This proposed method used non-linear regression classification algorithm for the effective fetus image classification process in this paper. The authors obtained 94.5% of average DS detection rate in ultrasound fetus images. Further, the k-fold validation approximation algorithm was also used in this work to validate the DS detection rate with respect to various set of test fetus ultrasound images. Chitkasaem Suwanrath et al. [16] measured the nasal bone length and its morphological parameters in order to assess the DS validation results in ultrasound fetus images. The morphological parameters of the segmented nasal bone have been compared with clinical results in order to perform unbias comparisons. The authors evaluated the results as 93.29% NTSe, 93.81NTSp and 93.29% NTAcc on Mendeley dataset fetus images The authors evaluated the results as 94.19% NTSe, 93.29 NTSp and 93.17% NTAcc on FMF dataset fetus images.

3. Proposed Methodologies

This research work proposes an automated ultrasound fetus image classification system using

DL algorithm. This proposed system receives the source ultrasound fetus image and the spatial domain pixels in this image have been converted into multi modal domain pixels using Gabor wavelet. Further, LBP has been computed from the multi domain image and these values have been fed into the proposed DL architecture to classify the source fetus image into either normal fetus or abnormal fetus.
Figure 2(a) is the proposed work flow of the ultrasound fetus image classifications in training and Figure 2(b) is the proposed work flow of the ultrasound fetus image classifications in testing.

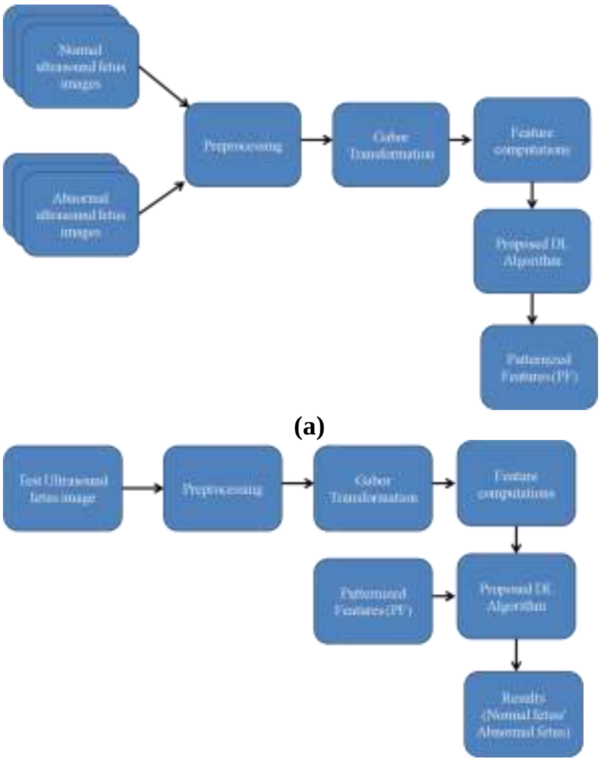

Figure 2 *(a) Ultrasound fetus image classifications (training) (b) Ultrasound fetus image classifications (testing)*

Preprocessing is a standard module in all proposed fetus image classification system which is used in this paper to perform the resize function (512*512-pixel image size) of the source fetus image to be suitable for further processing flow in the proposed fetus image classification system.

Gabor transform

The spatial properties of fetus images have been converted into multi domain properties using transformational approaches. The sensitivity and directionality of each pixel in the fetus image are improved in multi domain converted fetus image. Hence, the transformational approaches have been used for detecting the Down syndrome using the multi domain incorporated fetus image. There is lot of multi domain transformational approaches for the pixel conversion process such as Discrete Wavelet, Ridgelet, Contourlet and Gabor wavelet. Though all these transformational approaches available, the Gabor wavelet transformational approach has been used in this paper due to their higher sensitivity and directionality property. This Gabor wavelet transformational approach has been designed with two-dimensional Gaussian shaped kernel which is given in the following Equation.

$$gwk(x,y) = exp\left(\frac{-x^2+\gamma^2 y^2}{2\sigma^2}\right) * exp\left[i\left(2\pi\frac{x}{\rho}+\sigma\right)\right] \quad (1)$$

In this Equation, (x, y) represents the pixel coordination values corresponds to the standard deviation σ with respect to the frequency factor ρ.
This Gaussian shaped kernel has been multiplied by the ultrasound fetus image and the resultant image contains multi modal properties.
Figure 3 is the output image of the Gabor processed ultrasound fetus image.

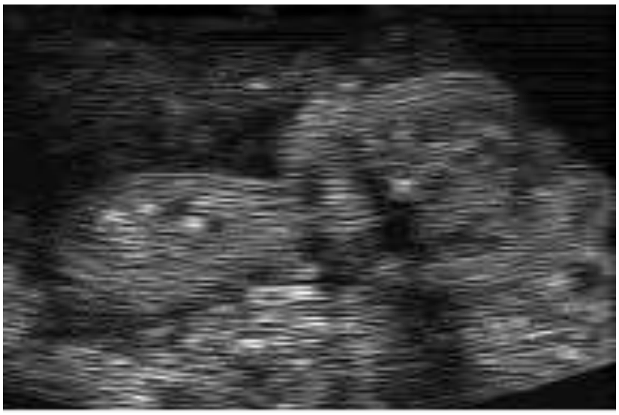

Figure 3 *Gabor processed ultrasound fetus image*

From the Gabor processed ultrasound fetus image, the LBP features have been estimated which produces similar size of the Gabor processed ultrasound fetus image in this work. This feature has been knows as the patternized features which are used to distinquish the normal fetus image from the abnormal fetus image through the classification module in the proposed fetus image classification system. The LBP of each pixel is computed by comparing their centreal value (placed 3 ×3 window over the center pixel, where the LBP has to be computed) with respect to the surrounding pixels in a 3 ×3 window.
Figure 4 (a) shows the pixel values in 3 ×3 window, Figure 4 (b) shows the binary image and Figure 4(c) shows the binary-decimal conversion. The following Equation has been used in this work to determine the LBP value of the single pixel in the Gabor processed ultrasound fetus image.

$$LBP(gp, gc) = \sum_{n=0}^{N-1} f(gp - gc) \times 2^n \quad (2)$$

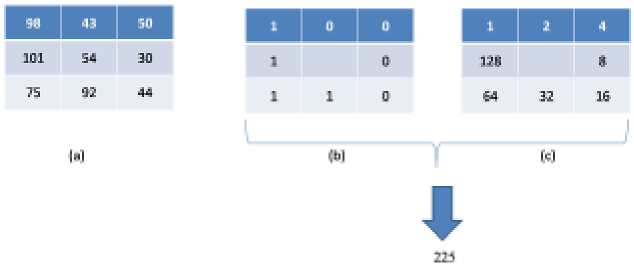

Figure 4 *(a) Pixel values in 3*3 window (b) Binary image (c) Binary-decimal conversion*

Whereas, N is the number of surrounding values in 3 ×3 computational window, gc is center pixel and gp is the surrounding pixels.

Figure 5 is the LBP fetus computational image and this LBP values have been computed for both normal fetus images and the abnormal fetus images and these values are further fed into the proposed DL classification module of the fetus image classification system.

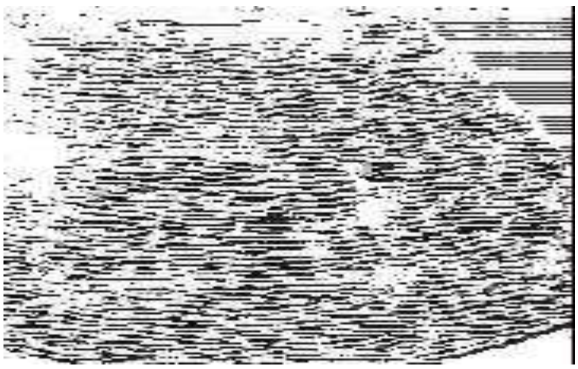

Figure 5 *LBP fetus computational image*

Fetus image classifications

Fetus image classification is an important process to identify the down syndrome disease. Machine learning algorithms have been used by many researchers to identify the down syndrome using ultrasound fetus images. Though the algorithms such as Support Vector Machine (SVM) and Adaptive Neuro Fuzzy Inference System (ANFIS) classifiers produced significant fetus image classification results, the fetus classification rate is not high for segmenting the nasal bone of the classified fetus image. Moreover, the fetus image classification rate is also low which affects the nasal bone segmentation process. Hence, DL algorithms have been used to detect the abnormal fetus image from the normal fetus image from the past two decades. These algorithms used standard DL architectures which consumed more processing time and also works on spatial feature pixels on the fetus images. Hence, there is a requirement for developing a higher efficient DL architecture for the effective fetus image classifications. Figure 6 is the proposed fetus image classification module (proposed Paternized Feature Deep Learning Network- PFDLN classifier).

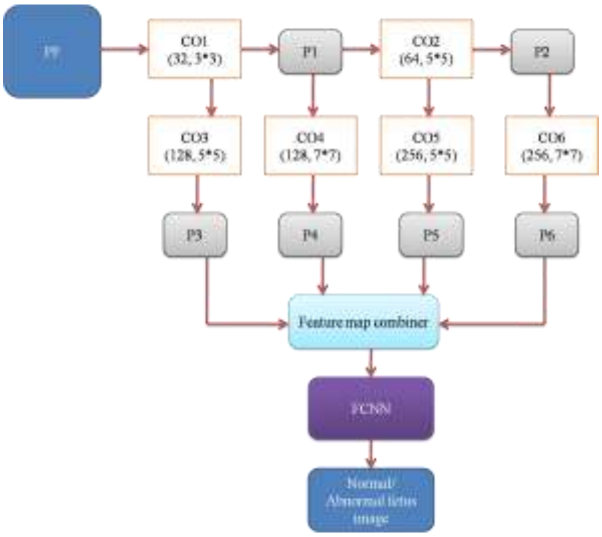

Figure 6 *Fetus image classification module (proposed Paternized Feature Deep Learning Network- PFDLN classifier)*

The fetus images have been classified into either normal or abnormal using the proposed DL algorithm in this work. The traditional DL algorithms require higher order computational layers which increased the system complexity during the classification of the images. Moreover, the tradional DL algorithm works directly on the spatial fetus images and produces the classification results. This study of limitations has been overcome by developing a Paternized Feature Deep Learning Network (PDFLN) classification module which is basically derived from the traditional AlexNet DL algorithm. This proposed PDFLN classification module works directly on the computed paternized features and produces the classification fetus results using minimum number of internal computational layers in this research work.

This proposed PDFLN classification module consist of six Convolutional layers (CO) and six pooling layers (P) as illustrated in Figure 6. The main purpose of CO layer is to produce larger number of features from the input values so that the classification results will be optimized. This CO layer has been operated by the two-dimensional kernel with varying its filter size. The input values of each CO layer has been convolved with this two dimensional kernel which produces the more set of features and these generated features are transferred to the next module through the P layer which reduces the size of the output of the CO layer. The P layer is operated by the pooling functions. The pooling functions are categorized into two types as Averaging Pool Function (APF) and Max Pool Function (MPF).

Figure 7(a) shows the functional working of APF where the average value has been taken for the values behind the encircled window. This may be generated new value during the pooling process which creates significant errors during the propagation of these values to the next layers. This drawback can be overcome by MPF which is illustrated in Figure 7(b). In MPF, the maximum value has been taken for the values behind the encircled window and hence it does not alter any value within this window during the entire process flow of the pooling function. This does not create significant errors during the propagation of these values to the next layers. Hence, MPF can be used in the proposed PDFLN classification module.

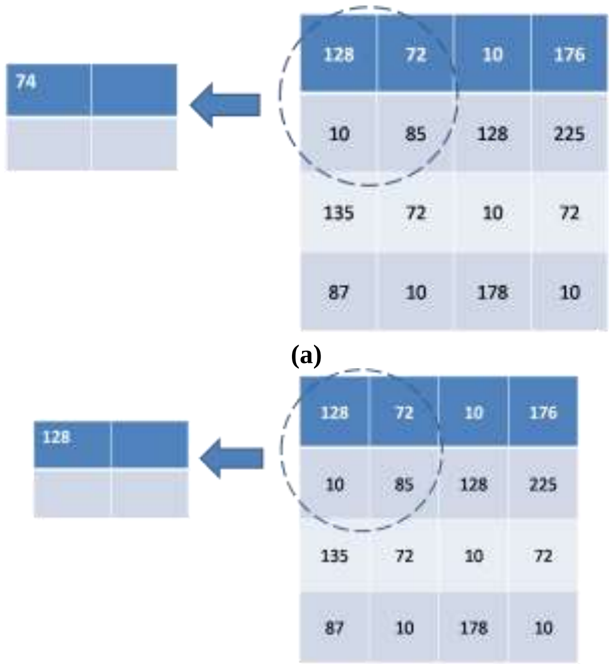

(b)

Figure 7 *(a) APF (b) MPF*

The PF is fed into CO1 which produces the output to the next layers P1 and CO3 simultaneously. The P1 reduces the output size using MPF and its output has been fed into CO2 and CO4 simultaneously. The output of CO2 has been fed into CO5 and P2 simultaneously. The output of P2 has been fed into CO6. The convolution process has been caried out in all four CO layers in second row of the proposed PDFLN classification module. Now, the output responses of all these four CO layers have been down sampled by passing them through the P layers as illustrated in Figure 5. Then, the output size reduced features have been combined by feature map combiner and its output values are passed to the Fully Connected Neural Networks (FCNN) layers. This FCNN have been structured by two internal modules as FCNN1 and FCNN2, where FCNN1 contains 4096 neurons and FCNN2 contains 2 neurons. The final module in FCNN produces the fetus image classification results as either normal fetus image or abnormal fetus image. Figure 8(a) is the classification results of normal fetus and Figure 8(b) is the classification results of the abnormal fetus.

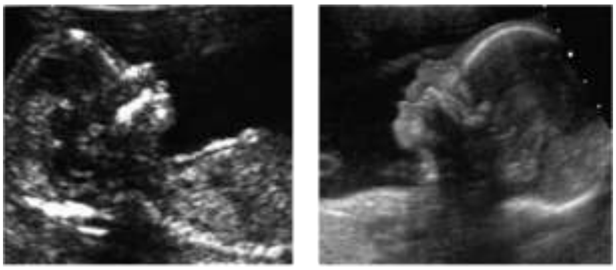

(a) (b)

Figure 8 *Fetus classification results (a) Normal fetus image (b) Abnormal fetus image (down syndrome case)*

In addition to the ultrasound fetus image classification process, morphological algorithm has been used to segment the nasal bone in this work.

4. Results and Discussions

This research work uses the ultrasound fetus images from two independent fetus datasets Mendeley [12] and Fetal Medicine Foundation (FMF) [13-19]. The Mendeley dataset contains 1528 two dimensional fetus ultrasound images which are acquired from the 1519 female persons. The fetus images have been collected from 11 to 14 weeks period of pregnancy. These ultrasound fetus images are collected from the Shenzhen people's hospital and all these ultrasound fetus images are stored in png format. These images are licenced by CC BY 4.0 and also this dataset have 156 additional ultrasound fetus images from the Longhua branch of the Shenzhen people's hospital. Moreover, the NT region has been marked in all these abnormal fetus images. Both abnormal and normal fetus ultrasound image size in this database is about 512 ×512 pixels.

In addition to the Mendeley dataset, FMF dataset consits of fetus ultra sound images which are aaquired from 11 to 13 weeks period of pregnancy in London, UK. This dataset contains 1250 fetus images and these fetus images have been categorized into 750 normal fetus images and 500 abnormal fetus images. Moreover, the NT region has been marked in all these abnormal fetus images in this FMF dataset. Both abnormal and normal fetus ultrasound image size in this database is about 256 ×256 pixels. The normal and abnormal fetus images detection performance has been analyzed with respect to the following functional index parameters. The Normal Featus Detection Index (NFDI) is defined as the ratio between the normal fetus images being correctly detected and the total normal fetus images. Similarly, The Abnormal Featus Detection Index

(AFDI) is defined as the ratio between the abnormal fetus images being correctly detected and the total abnormal fetus images. Both NFDI and AFDI have been measured in percentage and they are given in the below Equations.

$$Normal\ Fetus\ Detection\ Index\ (NFDI) = \frac{Normal\ fetus\ images\ being\ correctly\ detected}{Total\ normal\ fetus\ images} \times 100\% \quad (3)$$

$$Abnormal\ Fetus\ Detection\ Index\ (AFDI) = \frac{Abnormal\ fetus\ images\ being\ correctly\ detected}{Total\ abnormal\ fetus\ images} \times 100\% \quad (4)$$

In Mendeley dataset, the proposed fetus detection system obtains 98.6% NFDI by correctly detected 787 normal ultrasound fetus images by 798 normal fetus images and also obtains 98.7% AFDI by correctly detected 721 abnormal ultrasound fetus images by 730 abnormal fetus images. Hence, the average fetus detection rate on Mendeley dataset is about 98.65%. In FMF dataset, the proposed fetus detection system obtains 98.5% NFDI by correctly detected 739 normal ultrasound fetus images by 750 normal fetus images and also obtains 98.2% AFDI by correctly detected 491 abnormal ultrasound fetus images by 500 abnormal fetus images. Hence, the average fetus detection rate on FMF dataset is about 98.35%. The proposed NB region segmentation system has been analyzed with respect to the following mathematical Equations.

$$NB\ Segmented\ Sensitivity\ (NTSe) = TP/(TP + FN) \quad (5)$$

$$NB\ Segmented\ Specificity\ (NTSp) = TN/(TN + FP) \quad (6)$$

$$NB\ Segmented\ Accuracy\ (NTAcc) = (TP + TN)/(TP + FN + TN + FP) \quad (7)$$

Whereas, the NB and Non-NB region positively segmented NB pixels are represented by TP and TN, respectively and the NB and Non-NB region negatively segmented pixels are represented by FP and FN, respectively. Table 1 is the abnormal fetus NB region segmentation analysis on Mendeley dataset with respect to NBSe, NBSp and NBAcc. The proposed NB region segmentation system attains 98.44% NBSe, 98.63% NBSp and 98.62% NBAcc, for the set of 10 fetus images from the Mendeley dataset in this work. Figure 9 is the graphical illustrations on performance parameters (Mendeley dataset). Table 2 is the abnormal [20] fetus NB region segmentation analysis on FMF dataset with respect to NBSe, NBSp and NBAcc. The proposed NB region segmentation system attains 98.67% NBSe, 98.66% NBSp and 98.66% NBAcc, for the set of 10 fetus images [21] from the FMF dataset in this work. Figure 10 is the graphical illustrations on performance parameters (FMF dataset). Table 3 is the performance comparisons of NB region segmentation results between Mendeley and FMF datasets with respect to the abnormal fetus NB region segmentation parameters in this paper. Table 4 is the segmented NB region comparative analysis on Mendeley dataset fetus images with respect to state-of-the-art methods [8,10,11,13,16].

Table 1 *Abnormal fetus NB region segmentation analysis on Mendeley dataset*

Mendeley dataset abnormal fetus images	NB region segmentation analysis parameters in %		
	NBSe	**NBSp**	**NBAcc**
M1	98.3	98.4	98.9
M2	97.9	98.2	98.3
M3	98.1	98.9	98.1
M4	98.4	99.1	99.4
M5	98.2	99.3	99.1
M6	99.3	98.9	98.7
M7	98.7	98.3	98.3
M8	98.5	98.1	98.9
M9	98.1	98.7	98.4
M10	98.9	98.4	98.1
Mean	**98.44**	**98.63**	**98.62**

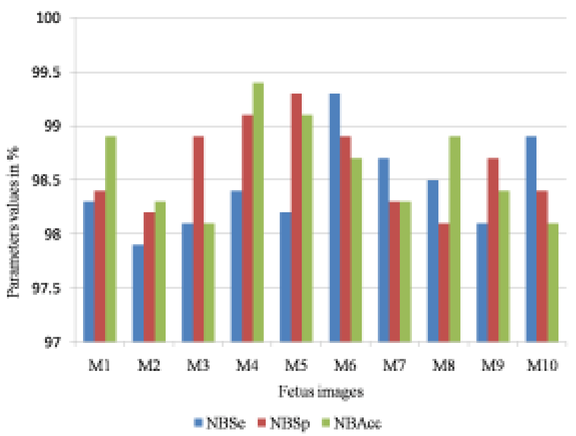

Figure 9 *Graphical illustrations on performance parameters (Mendeley dataset)*

Table 2 *Abnormal fetus NB region segmentation analysis on FMF dataset*

FMF dataset abnormal fetus images	NB region segmentation analysis parameters in %		
	NBSe	**NBSp**	**NBAcc**
F1	98.7	98.4	98.3
F 2	98.3	98.8	98.9
F 3	99.1	98.9	98.2
F 4	99.4	99.1	98.6
F 5	98.2	98.4	98.9
F 6	98.9	98.3	99.1
F 7	98.4	98.8	99.3
F 8	98.3	98.5	98.6
F 9	98.1	98.3	98.4
F 10	99.3	99.1	98.3
Mean	**98.67**	**98.66**	**98.66**

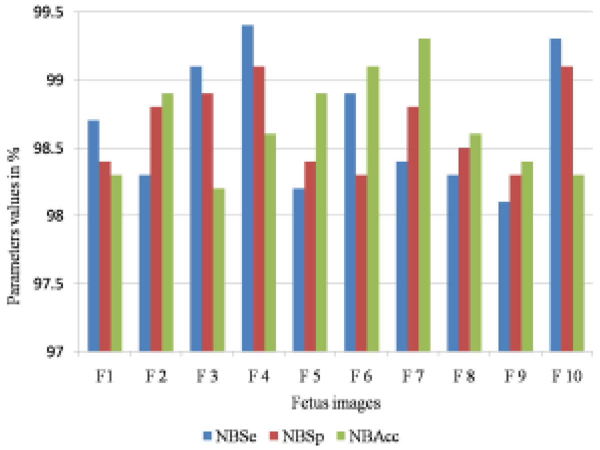

Figure 10 *Graphical illustrations on performance parameters (FMF dataset)*

Table 3. *Performance comparisons of NB region segmentation results between Mendeley and FMF datasets*

Abnormal fetus NB region segmentation parameters	Mendeley dataset	FMF dataset
NBSe (%)	98.44	98.67
NBSp (%)	98.63	98.66
NBAcc (%)	98.62	98.66

Table 4 *Segmented NB region comparative analysis on Mendeley dataset fetus images with respect to state-of-the-art methods*

Methods	NB region segmentation analysis parameters in %		
	NBSe	**NBSp**	**NBAcc**
Proposed work	98.44	98.63	98.62
[8]	96.2	96.65	96.38
[10]	96.1	96.38	96.12
[13]	95.29	95.27	95.98
[11]	94.65	94.87	95.01
[16]	93.29	93.81	93.29

Table 5 is the segmented [22] NB region comparative analysis on FMF dataset fetus images with respect to state-of-the-art methods [8,10,11,13,16,23]. Deep learning is important and was used in different fields [24-35].

5. Conclusions

The fully automated ultrasound fetus image classification system has been proposed in this paper for downsyndrome detection. In Mendeley dataset, the proposed fetus detection system obtains 98.6% NFDI by correctly detected 787 normal ultrasound fetus images by 798 normal fetus images and also obtains 98.7% AFDI by correctly detected 721 abnormal ultrasound fetus images by 730 abnormal

Table 5 *Segmented NB region comparative analysis on FMF dataset fetus images with respect to state-of-the-art methods*

Methods	NB region segmentation analysis parameters in %		
	NBSe	**NBSp**	**NBAcc**
Proposed work	**98.67**	**98.66**	**98.66**
[8]	97.10	97.67	97.59
[10]	96.67	96.02	96.28
[13]	95.29	95.67	95.46
[11]	94.98	94.39	94.29
[16]	94.19	93.29	93.17

fetus images. Hence, the average fetus detection rate on Mendeley dataset is about 98.65%. In FMF dataset, the proposed fetus detection system obtains 98.5% NFDI by correctly detected 739 normal ultrasound fetus images by 750 normal fetus images and also obtains 98.2% AFDI by correctly detected 491 abnormal ultrasound fetus images by 500 abnormal fetus images. Hence, the average fetus detection rate on FMF dataset is about 98.35%. The proposed NB region segmentation system attains 98.44% NB Se, 98.63% NB Sp and 98.62% NB Acc, for the Mendeley dataset in this work.

The proposed NB region segmentation system attains 98.67% NB Se, 98.66% NB Sp and 98.66% NB Acc, for the set of for the FMF dataset in this work. In future, the NT will be detected and segmented using DL algorithm and its morphological properties will be analsyzed for its automated diagnosis process.

Author Statements:

- **Ethical approval:** The conducted research is not related to either human or animal use.
- **Conflict of interest:** The authors declare that they have no known competing financial interests or personal relationships that could have appeared to influence the work reported in this paper
- **Acknowledgement:** The authors declare that they have nobody or no-company to acknowledge.
- **Author contributions:** The authors declare that they have equal right on this paper.
- **Funding information:** The authors declare that there is no funding to be acknowledged.
- **Data availability statement:** The data that support the findings of this study are available on request from the corresponding author. The data are not publicly available due to privacy or ethical restrictions.

References:

[1]Ghabri, H., Alqahtani, M.S., Ben Othman, S. et al. (2023). Transfer learning for accurate fetal organ classification from ultrasound images: a potential tool for maternal healthcare providers. *Sci Rep* 13, 17904.

[2]Burgos-Artizzu, X. P. *et al.* (2020). Evaluation of deep convolutional neural networks for automatic classification of common maternal fetal ultrasound planes. *Sci. Rep.* 10, 10200.

[3]Kaplan, E. et al. (2022). PFP-LHCINCA: Pyramidal fixed-size patch-based feature extraction and chi-square iterative neighborhood component analysis for automated fetal sex classification on ultrasound images. *Contrast Media Mol. Imaging*, e6034971.

[4]Jordina Torrents-Barrena, Núria Monill ,(2021). Assessment of Radiomics and Deep Learning for the Segmentation of Fetal and Maternal Anatomy in Magnetic Resonance Imaging and Ultrasound, *Academic Radiology*, 28(2);173-188.

[5]Burgos-Artizzu, X.P., Coronado-Gutiérrez, D., Valenzuela-Alcaraz, B. et al. (2020). Evaluation of deep convolutional neural networks for automatic classification of common maternal fetal ultrasound planes. *Sci Rep* 10;10200.

[6]Tamilarasi M, Kumarganesh S, K. Martin Sagayam, and Andrew J, (2024). Detection and Segmentation of Glioma Tumors Utilizing a UNet Convolutional Neural Network Approach with Non-Subsampled Shearlet Transform *Journal of Computational Biology*, 31(8);1-15, https://doi.org/10.1089/cmb.2023.0339.

[7]Hom, B., Boyd, N.K., Vogel, B.N. et al. (2024). Down Syndrome and Autoimmune Disease. *Clinic Rev Allerg Immunol*, 1(1);1-14.

[8]Aijaz Ahmad Reshi, Shabana Shafi, Irfan Qayoom, Maria Wani, Shahida Parveen and Ajaz Ahmad (2024). Deep Learning based architecture for Down syndrome assessment during early pregnancy using fetal ultrasound images. *International Journal of Experimental Research and Review*, 38;182-193.

[9]Thiyaneswaran B, Anguraj K, et al., (2021), Early Detection of Melanoma Images using gray level co-occurrence matrix Features and Machine Learning Techniques for Effective Clinical Diagnosis *International Journal of Imaging Systems and technology*, 31(2);682-694. https://doi.org/10.1002/ima.22514

[10]Chengyu Wang , Limin Yu , Jionglong Su , Trevor Mahy , Valerio Selis , Chunxiao Yang , Fei Ma, (2023). Down Syndrome detection with Swin Transformer architecture, *Biomedical Signal Processing and Control*, 86;105199.

[11]M. C. Thomas and S. P. Arjunan, (2022). Deep learning measurement model to segment the nuchal translucency region for the early identification of down syndrome, *Meas. Sci. Rev*., 22(4);187–192. DOI: 10.2478/msr-2022-0023

[12]P. Elayaraja, Kumarganesh S, K. Martin Sagayam & J. Andrew, (2024), An automated cervical cancer diagnosis using genetic algorithm and CANFIS approaches. *International Journal of Technology and Health Care*, 32(4);1-17, DOI**:** 10.3233/THC-230926

[13]N. H. Phung, C. T. Nguyen, T. K. Tran, T. T. H. Truong, D. C. Tran, T. T. Nguyen, and D. H. Do, (2023). A combination of multi-branch CNN and feature rearrangement for down syndrome prediction, *in Proc. Int. Conf. Artif. Intell. Inf. Commun. (ICAIIC)*, Feb. 2023, pp. 1–6.

[14]Senthilkumar T, Kumarganesh S, Sivakumar P and Periyarselvam K, (2022). Primitive detection of Alzheimer's disease using neuroimaging: A progression model for Alzheimer's disease: Their applications, benefits, and drawbacks" *Journal of Intelligent & Fuzzy Systems*, 43(4);4431-4444, DOI: 10.3233/JIFS-220628.

[15]Kumarganesh. S and M. Suganthi, (2016), An Efficient Approach for Brain Image (Tissue) Compression Based on the Position of the Brain Tumor *International Journal of Imaging Systems and technology*, 26(4);237– 242, DOI:10.1002/ima.22194

[16]Chitkasaem Suwanrath, Ninlapa Pruksanusak, Ounjai Kor-anantakul, Thitima Suntharasaj, Tharangrut Hanprasertpong and Savitree Pranpanus, (2013). Reliability of fetal nasal bone length measurement at 11–14 weeks of gestation, *BMC Pregnancy and Childbirth* 13;7. doi: 10.1186/1471-2393-13-7

[17]Cui, Chen; Dong, Fajin (2022), "Dataset for Fetus Framework", Mendeley Data, V1.

[18]Mendeley dataset: https://data.mendeley.com/datasets/n2rbrb9t4f/1

[19]FMF **dataset**: https://fetalmedicine.org/education/fetal-abnormalities.

[20]Sasikala, S., Sasipriya, S., & Maheshwari, U. (2022). Soft Computing based Brain Tumor Categorization with Machine Learning Techniques. *In 2022 International Conference on Advanced Computing Technologies and Applications (ICACTA)* (pp. 1-9).

[21]Rajendran, U. M., & Paulchamy, J. (2021). Analysis and classification of gait characteristics. *Iconic Research and Engineering Journals*, 4(12).

[22]Maheshwari, R. U., Paulchamy, B., Pandey, B. K., & Pandey, D. (2024). Enhancing Sensing and Imaging Capabilities Through Surface Plasmon Resonance for Deepfake Image Detection. *Plasmonics*, 1-20. DOI:10.1007/s11468-024-02492-1

[23]Maheshwari, R. U., Jayasutha, D., Senthilraja, R., & Thanappan, S. (2024). Development of Digital Twin Technology in Hydraulics Based on Simulating and Enhancing System Performance. *Journal of Cybersecurity & Information Management*, 13(2) DOI:10.54216/JCIM.130204

[24]Ay, S. (2024). Vehicle Detection And Vehicle Tracking Applications On Traffic Video Surveillance Systems: A systematic literature review. *International Journal of Computational and Experimental Science and Engineering*, 10(4);1059-1068. https://doi.org/10.22399/ijcesen.629

[25]Nagalapuram, J., & S. Samundeeswari. (2024). Genetic-Based Neural Network for Enhanced Soil Texture Analysis: Integrating Soil Sensor Data for

Optimized Agricultural Management. *International Journal of Computational and Experimental Science and Engineering*, 10(4);962-970. https://doi.org/10.22399/ijcesen.572
[26]Machireddy, C., & Chella, S. (2024). Reconfigurable Acceleration of Neural Networks: A Comprehensive Study of FPGA-based Systems. *International Journal of Computational and Experimental Science and Engineering*, 10(4);1007-1014. https://doi.org/10.22399/ijcesen.559
[27]Priti Parag Gaikwad, & Mithra Venkatesan. (2024). KWHO-CNN: A Hybrid Metaheuristic Algorithm Based Optimzed Attention-Driven CNN for Automatic Clinical Depression Recognition. *International Journal of Computational and Experimental Science and Engineering*, 10(3);491-506. https://doi.org/10.22399/ijcesen.359
[28]Rama Lakshmi BOYAPATI, & Radhika YALAVARTHI. (2024). RESNET-53 for Extraction of Alzheimer's Features Using Enhanced Learning Models. *International Journal of Computational and Experimental Science and Engineering*, 10(4);879-889. https://doi.org/10.22399/ijcesen.519
[29]S.D.Govardhan, Pushpavalli, R., Tatiraju.V.Rajani Kanth, & Ponmurugan Panneer Selvam. (2024). Advanced Computational Intelligence Techniques for Real-Time Decision-Making in Autonomous Systems. *International Journal of Computational and Experimental Science and Engineering*, 10(4);928-937. https://doi.org/10.22399/ijcesen.591
[30]Rakesh Jha, & Singh, M. K. (2024). Analysing the Impact of Social Influence on Electric Vehicle Adoption: A Deep Learning-Based Simulation Study in Jharkhand, India. *International Journal of Computational and Experimental Science and Engineering*, 10(4);639-646. https://doi.org/10.22399/ijcesen.371
[31]Serap ÇATLI DİNÇ, AKMANSU, M., BORA, H., ÜÇGÜL, A., ÇETİN, B. E., ERPOLAT, P., … ŞENTÜRK, E. (2024). Evaluation of a Clinical Acceptability of Deep Learning-Based Autocontouring: An Example of The Use of Artificial Intelligence in Prostate Radiotherapy. *International Journal of Computational and Experimental Science and Engineering*, 10(4);1181-1186. https://doi.org/10.22399/ijcesen.386
[32]Suneetha Madduluri, & T. Kishorekumar. (2024). Multimodal Biometric Authentication System for Military Weapon Access: Face and ECG Authentication. *International Journal of Computational and Experimental Science and Engineering*, 10(4);952-961. https://doi.org/10.22399/ijcesen.565
[33]PATHAPATI, S., N. J. NALINI, & Mahesh GADIRAJU. (2024). Comparative Evaluation of EEG signals for Mild Cognitive Impairment using Scalograms and Spectrograms with Deep Learning Models. *International Journal of Computational and Experimental Science and Engineering*, 10(4);859-866. https://doi.org/10.22399/ijcesen.534
[34]J Jeysudha, K. Deiwakumari, C.A. Arun, R. Pushpavalli, Ponmurugan Panneer Selvam, & S.D. Govardhan. (2024). Hybrid Computational Intelligence Models for Robust Pattern Recognition and Data Analysis . *International Journal of Computational and Experimental Science and Engineering*, 10(4);1032-1040. https://doi.org/10.22399/ijcesen.624
[35]U. S. Pavitha, S. Nikhila, & Mohan, M. (2024). Hybrid Deep Learning Based Model for Removing Grid-Line Artifacts from Radiographical Images. *International Journal of Computational and Experimental Science and Engineering*, 10(4);763-774. https://doi.org/10.22399/ijcesen.514